Atmos. Meas. Tech. Discuss., 8, 3525–3570, 2015
www.atmos-meas-tech-discuss.net/8/3525/2015/
doi:10.5194/amtd-8-3525-2015

Atmospheric Measurement Techniques Discussions

Aerosol mass spectrometry: particle–vaporizer interactions and their consequences for the measurements

F. Drewnick[1], **J.-M. Diesch**[1], **P. Faber**[1], **and S. Borrmann**[1,2]

[1]Max Planck Institute for Chemistry, Particle Chemistry Department, Hahn-Meitner-Weg 1, 55128 Mainz, Germany
[2]Johannes Gutenberg University, Institute for Atmospheric Physics, J.-J.-Becherweg 21, 55128 Mainz, Germany

Received: 12 February 2015 – Accepted: 10 March 2015 – Published: 2 April 2015

Correspondence to: F. Drewnick (frank.drewnick@mpic.de)

Published by Copernicus Publications on behalf of the European Geosciences Union.

Abstract

The Aerodyne Aerosol Mass Spectrometer (AMS) is a frequently used instrument for on-line measurement of the ambient sub-micron aerosol composition. With the help of calibrations and a number of assumptions on the flash vaporization and electron impact ionization processes this instrument provides robust quantitative information on various ambient aerosol components. However, when measuring close to certain anthropogenic sources or in marine environments, several of these assumptions may not be met and measurement results might easily be misinterpreted.

Here we discuss various aspects of the interaction of aerosol particles with the AMS tungsten vaporizer and the consequences for the measurement results: semi-refractory components, i.e. components that vaporize but do not flash vaporize at the vaporizer and ionizer temperatures, like metal halides (e.g. chlorides, bromides or iodides of Al, Ba, Cd, Cu, Fe, Hg, K, Na, Pb, Sr, Zn) can be measured semi-quantitatively despite their relatively slow vaporization from the vaporizer. Even though non-refractory components (e.g. NH_4NO_3 or $(NH_4)_2SO_4$) vaporize quickly, their differences in vaporization kinetics can result in undesired biases in ion collection efficiency in the measurements. Chemical reactions with water vapor and oxygen from the aerosol flow can have an influence on the mass spectra for certain components (e.g. NH_4NO_3, $(NH_4)_2SO_4$, organic species). Finally, chemical reactions of the aerosol with the vaporizer surface can result in additional signals in the mass spectra (e.g. WO_2Cl_2-related signals from particulate Cl) and in conditioning or contamination of the vaporizer with potential memory effects influencing the mass spectra of subsequent measurements.

Laboratory experiments that investigate these particle–vaporizer interactions are presented and are discussed together with field results showing that measurements of typical continental or urban aerosols are not significantly affected while laboratory experiments, measurements close to anthropogenic sources or in marine environments can be biased by these effects.

AMTD
8, 3525–3570, 2015

1 Introduction

Flash vaporization in combination with mass spectrometry is used since decades for the analysis of thermally fragile (e.g. Lincoln, 1965; Chinn and Lagow, 1984) or environmental (e.g. Leeuw et al., 1986) samples with little or no pre-treatment needed. For the measurement of inorganic (e.g. Roberts, 1976; Stolzenburg et al., 2000, 2003) and organic (Lim et al., 2003) aerosol components flash vaporization is often used in combination with optical gas analyzers. Also in on-line aerosol mass spectrometry flash vaporization was used from the very beginning on in combination with surface ionization (Davis, 1973; Stoffels and Lagergren, 1981) and with subsequent electron impact ionization (Allen and Gould, 1981; Sinha et al., 1982). Today, one of the most widespread instruments for on-line analysis of the sub-micron aerosol is the Aerodyne Aerosol Mass Spectrometer (AMS), which also applies flash vaporization of the aerosol particles and subsequent electron impact ionization of the vapor (Jayne et al., 2000). Common to these applications is the general assumption that flash vaporization quickly converts the solid sample material into a vapor without alteration – besides thermal decomposition – of the sample.

In the AMS the aerosol particles are – together with a small fraction (10^{-7}) of the carrier gas – directed onto the tungsten vaporizer, typically heated to a temperature of 550–600 °C. Non-refractory material flash vaporizes and the emerging vapor is electron impact ionized (70 eV) for subsequent analysis with a quadrupole (Jayne et al., 2000) or a time-of-flight (Drewnick et al., 2005; DeCarlo et al., 2006) mass spectrometer. In addition to the measurement of the aerosol beam ("*beam open*" mass spectrum) also the instrument background is measured with the aerosol beam blocked ("*beam closed*" mass spectrum). The particle contribution is calculated from the difference of both measurements ("*difference*" spectrum), assuming that all particle components vaporize quickly compared to the *beam open*/*beam closed* cycle length (Jimenez et al., 2003). For calculation of mass concentrations of species from the *difference* spectrum each individual m/z is associated with one or several of these species (Allan et al., 2004b).

AMTD
8, 3525–3570, 2015

For the standard analysis of the unit mass resolution spectra these associations are hard-coded in the "*frag table*". Measurements with the high-resolution AMS (HR-ToF-AMS, DeCarlo et al., 2006) allow the quantification of individual signals in the spectra with certain elemental compositions (Aiken et al., 2007; Canagaratna et al., 2015).

For measurements of the continental or urban background aerosol the assumptions behind this procedure are typically well met and the AMS provides robust quantitative information on the sub-micron aerosol composition (Canagaratna et al., 2007). However, under certain conditions, e.g. when measuring close to anthropogenic sources or in the marine environment the limitations of these assumptions are sometimes reached and the standard analysis could result in misinterpretation of the mass spectra. Nevertheless, under such conditions additional information extending beyond the standard AMS species can often be retrieved from the mass spectra: in measurements of the marine aerosol NaCl, which is generally claimed to be refractory and therefore not measurable with the AMS, was unambiguously measured with this instrument (Zorn et al., 2008; Ovadnevaite et al., 2012; Schmale et al., 2013). In the measurements of fireworks (Drewnick et al., 2006) and hand flare emissions (Faber et al., 2013) several metal-containing species (e.g. with Fe, Mg, K, Cu, Li, Na) and their fragments have been identified, albeit not quantified in the mass spectra. Close to a steelworks plant elemental sulfur particles were identified in AMS spectra with the help of co-located single particle mass spectrometric measurements (Dall'Osto et al., 2012). Finally, during a few AMS measurements in urban environments metals or metal-containing compounds including Rb, Cs, Cu, Zn, As, Se, Sn, Sb or Pb have been found in the aerosol mass spectra (Takegawa et al., 2009; Salcedo et al., 2010, 2012).

For some of these "unusual" compounds an unusual vaporization behavior was observed with vaporization extending over prolonged time intervals. During the measurement of increased aerosol concentrations, increased background (*beam closed*) concentrations have even been observed for the standard non-refractory AMS species (Drewnick et al., 2009). For less volatile or very "sticky" species the background fraction increases (e.g. Salcedo et al., 2010, 2012), sometimes up to a level that they mainly

AMTD
8, 3525–3570, 2015

act as a contamination of the mass spectra, like it was observed for bromine and iodine even months after their measurement in the laboratory (e.g. Zorn et al., 2008; Drewnick et al., 2009). In order to extract quantitative information on such species different approaches have been applied. These include the determination of relative ionization efficiencies (RIE), either by comparison with external measurements (Drewnick et al., 2006) or by laboratory experiments (Ovadnevaite et al., 2012), or modelling of the mass concentration of a semi-refractory species from the *beam open* and *beam closed* signals of the mass spectra (Salcedo et al., 2010).

In order to better understand the processes occurring when particles vaporize from the AMS vaporizer we have performed various experiments in the laboratory. Some of these experiments were focused on the vaporization of individual non-refractory particles, others on the kinetics of particle vaporization of semi-refractory species. In further experiments the influence of the relative humidity and oxygen in the carrier gas on chemical reactions at the vaporizer was investigated. Additionally, chemical reactions of the aerosol with the vaporizer itself and their influence on the resulting mass spectra have been evaluated. For clarity reasons we divided this manuscript into two main sections dealing with the kinetics of particle vaporization (Sect. 3) and with chemical reactions at the vaporizer (Sect. 4), respectively. Subsequently we discuss the significance of the findings and their potential impact on the measurements in general and for certain measurement conditions.

2 Measurement setup

All laboratory experiments were performed using a similar setup (Fig. 1). Aerosols of known composition were generated by atomizing a solution of the individual components in ultra-pure water (18 MΩ cm, UHQ II, ELGA Purelab) using a constant output atomizer (TSI, model 3076). Subsequently, the aerosol particles were dried in a silica gel diffusion aerosol dryer. For measurements with defined relative humidity the aerosol was passed through a dilution and conditioning chamber where it was mixed

AMTD
8, 3525–3570, 2015

with particle-free air of known relative humidity (RH), resulting in an aerosol RH of 1.5 to 85 %. For several of the measurements a DMA (Differential Mobility Analyzer, TSI, model 3081) was used to select particles of a certain diameter or to switch on and off the particle stream without changing any other parameters in the experimental setup. Finally, the aerosol flow was split and directed into the AMS and in parallel into a CPC (Condensation Particle Counter, TSI, model 3025a) for parallel number concentration measurement. In addition, measurements using argon as carrier and dilution gas were performed to investigate the influence of oxygen in the aerosol onto the resulting mass spectra. In all cases, after changing the carrier gas or the aerosol relative humidity, sufficient time to allow the system to equilibrate (several tens of minutes up to several hours) was given before the measurements under the respective conditions were performed.

All chemicals used for the measurements presented here were of typical analytical purity (97 % up to > 99 %) and were purchased from several suppliers of laboratory chemicals (Fluka, Carl Roth GmbH, Sigma-Aldrich, and Merck KGaA).

For the aerosol measurements two different aerosol mass spectrometers were used. For the single particle vaporization event measurements a C-ToF-AMS was applied, which allows very frequent sampling of the ion flow from the vaporizer/ionizer into the mass spectrometer. These measurements were performed with an ion extractor pulser frequency of 83 kHz (12 µs pulser period) in BFSP mode (Brute Force Single Particle mode: non-averaged Particle Time-Of-Flight (PTOF) mode, i.e. separated collection of a series of consecutive mass spectra without averaging). For all other measurements a HR-ToF-AMS was used, which does not allow such a high ion sampling rate (pulser frequency 20 kHz ∼ 50 µs pulser period) but provides more detailed information on the identity of individual ion peaks from the high resolution mass spectra. For these measurements mainly the mass spectrum (MS) mode was used. The length of the *beam open*/*beam closed* cycles varied, depending on the respective type of measurement. If not otherwise stated measurements were performed with the standard vaporizer temperature of 550–600 °C.

AMTD
8, 3525–3570, 2015

3 Particle vaporization kinetics

3.1 Single particle vaporization events

All AMS measurements are based on the vaporization of individual particles from the AMS vaporizer, a porous tungsten rod with an inverted cone shape (both for improved collection efficiency of the particles), that can be heated up to approximately 800 °C (typical operation temperature: 550–600 °C). Ammonium nitrate (NH_4NO_3) and ammonium sulfate ($(NH_4)_2SO_4$) are the most common inorganic non-refractory species measured with the AMS on a regular basis. Here, single particle vaporization events for these species have been investigated in some detail in several experiments. For this purpose a C-ToF-AMS was operated at high (83 kHz) pulser frequency in BFSP mode.

In Fig. 2a the typical temporal evolution of ammonium nitrate single particle vaporization events is depicted for three ions associated with this species. The amount of ammonium and nitrate within the particle is proportional to the integrated area under the peaks related to the respective species. However, in addition to differences in single particle vaporization event peak area also differences in peak width and shape can be seen for the three ions. This is likely associated with the thermal decomposition processes occurring during the particle vaporization event:

$$NH_4NO_3 \rightleftharpoons NH_3\uparrow + HNO_3\uparrow \quad \text{(R1)}$$

$$4\,HNO_3 \rightleftharpoons 4\,NO_2 + 2\,H_2O + O_2 \quad \text{(R2)}$$

$$NO_2 \rightleftharpoons NO + 1/2\,O_2 \quad \text{(R3)}$$

While generally, these reactions as well as the reactions presented further below are equilibrium reactions, under the conditions in the AMS they will be limited by the expansion of the evolving vapor from the vaporizer into the surrounding vacuum. In the early phase of this process abundant collisions between vapor components also allow the back reactions, however, this will be decreasingly the case in later phases of this expansion. Molecules generated during the thermal decomposition processes are ion-

AMTD
8, 3525–3570, 2015

ized by electron impact and as a consequence fragment into the various ions observed in the mass spectra. Within these ions, m/z 30 (NO^+) is from NO, NO_2 and HNO_3, while m/z 46 (NO_2^+) is from NO_2 and HNO_3 only (Friedel at al. 1953). The longer appearance of the m/z 30 signal – after the other signals already have decayed (Fig. 2a) – suggests that the NO molecules, as end products of Reactions (R1) to (R3), survive the high temperature condition longest and/or have the longest potential to stay in the ionizer volume by adsorption/desorption to the ionizer walls.

This effect – of longer vaporization event length of the m/z 30 ion (46 µs full width half maximum, FWHM) compared to the m/z 46 ion (29 µs) – can become relevant if the sampling frequency of the ions (i.e. the pulser frequency of the ToF-MS) is small and the pulser period is in the order of the particle vaporization event length. With event lengths in the order of 25 to 40 µs FWHM for many of the ions, this is the case for measurements with the HR-ToF-AMS. As a consequence of the less frequent sampling of the ions into the MS not only a larger fraction of the ions is missed (i.e. the measured number of ions per particle (IPP) is reduced, Fig. 2b), but also the chance to miss a large fraction of the shorter m/z 46 peak is significantly larger compared to that of the longer m/z 30 peak (Fig. 2b). This will result in a change in the fragmentation pattern of ammonium nitrate (m/z 30 to m/z 46 ratio) when the pulser frequency changes. Therefore – and due to the IPP changes – measurements should always be performed with a pulser frequency as high as possible and at the same pulser frequency as was used during calibration measurements.

For ammonium sulfate generally slightly longer particle vaporization events are observed, compared to ammonium nitrate (Fig. 2c). This difference can possibly be explained by the higher vaporization temperature of $(NH_4)_2SO_4$ compared to NH_4NO_3. The even longer vaporization event length of the m/z 64 and m/z 48 signals compared to those of m/z 80, 81 and 98 are also associated with the processes during particle

AMTD
8, 3525–3570, 2015

vaporization:

$$(NH_4)_2SO_4 \rightleftharpoons 2\,NH_3\uparrow + H_2SO_4\uparrow \quad \text{(R4)}$$

$$H_2SO_4 \rightleftharpoons H_2O + SO_3 \quad \text{(R5)}$$

$$SO_3 \rightleftharpoons SO_2 + 1/2\,O_2 \quad \text{(R6)}$$

The ions at m/z 81 (HSO_3^+) and 98 ($H_2SO_4^+$) are only generated from H_2SO_4 and those at m/z 80 (SO_3^+) from H_2SO_4 and SO_3, while the ions at m/z 48 (SO^+) and 64 (SO_2^+) are also generated from the emerging SO_2, which is the final decomposition product according to Reactions (R4) to (R6). Also these differences in vaporization event length have the potential to cause changes in fragmentation patterns when changing the pulser frequency of the mass spectrometer.

Flash vaporization assumes "immediate" conversion of a solid or a liquid into a vapor. The finite length of the vaporization events (Fig. 2c) is a consequence of several factors like the time to heat the whole particle up to a temperature where it vaporizes, the expansion and self-cleaning time constants for the vapor in the ionizer volume, i.e. the time it takes for the vapor to be removed from the ionizer volume which can be prolonged as a consequence of potential adsorption and desorption processes on the ionizer walls, and ion sampling time constants. Since several of these factors depend on the temperature of the vaporizer, measurements of vaporization event length as a function of vaporizer temperature have been performed.

For low vaporizer temperatures an exponential decrease of vaporization event length with increasing vaporizer temperature is found (Fig. 2d, logarithmic scale). Above a threshold temperature, which depends on the volatility of the species under investigation, no further decrease of vaporization event length with increasing vaporizer temperature is observed. This threshold temperature is about 310 °C for NH_4NO_3, 400 °C for $(NH_4)_2SO_4$, and 450 °C for NH_4Cl (not shown). In order to be able to measure particle size distributions which are not broadened by slow vaporization of the particles off the vaporizer, its temperature must be set above this threshold value. For example for particle size calibrations commonly polystyrene latex (PSL) particles are used,

AMTD
8, 3525–3570, 2015

which need significantly higher vaporizer temperatures (≥ 750 °C) for sufficiently quick vaporization.

3.2 Vaporization kinetics of non-refractory species

While non-refractory species like ammonium nitrate and ammonium sulfate vaporize quickly and generate short ion pulses when the particles hit the vaporizer, an increase in nitrate or sulfate instrument background with subsequent increase in detection limit for these species has been observed when measuring enhanced concentrations of such aerosol components (Drewnick et al., 2009).

To investigate the kinetics of particle vaporization in more detail, experiments have been conducted where the *beam open* and *beam closed* intervals have been extended to approximately 17 min each and the mass concentration was measured during this time with best possible time resolution (~ 5 s, i.e. one second sampling time, four seconds saving time). In Fig. 3a the temporal evolution of the m/z 18 (H_2O^+), 30 (NO^+) and 46 (NO_2^+) signals is shown over three complete *beam open*/*beam closed* cycles of the measurement of ammonium nitrate particles. While for the nitrate-related ions a very quick increase and decrease of the measured concentrations is observed, the water-related signal shows a slower, more gradual approach to the final levels. In addition, for water even after 17 min of *beam closed* measurements still a significant signal background is found (~ 56 % of signal maximum).

Within the first 10 s of the blocking of the aerosol beam the m/z 30 signal intensity decreases to ~ 2 % of its previous value; for the m/z 46 signal this decrease is even down to ~ 0.4 %. During the following 17 min an additional decrease by another factor of 4–5 is observed for both ions. This means that the m/z 30 to m/z 46 ratio changes from about 2.9 (close to the 3 : 1 ratio of these ions for pure NO_2, Friedel et al., 1953) during the aerosol measurement very quickly to a value of 20–25 (i.e., signal dominated by NO) during the background measurement. When the aerosol beam is measured again the observed signals increase very quickly, reaching ~ 95 % of their final value within the first 5 s cycle. A significantly different behavior is found for the m/z 18 signal

AMTD
8, 3525–3570, 2015

which in parts stems from the thermal decomposition of the nitric acid (Reactions R1 and R2). During the first 10 s of the background measurement this signal decreases to 69 % of its initial value, while it decreases by another 13 % during the following 17 min. Also the signal increase after re-opening the particle beam is much slower. After 10 s only 50 % of the previous decrease is recovered.

These results suggest that during the measurement of ammonium nitrate aerosol a small fraction of the nitric acid from the thermal decomposition of the particle material (R1) is actually ionized and measured in the mass spectrometer, while the majority of the material further decomposes into NO_2 (R2) before the measurement. As already observed in the single particle vaporization events, NO_2 quickly decomposes into NO and oxygen (R3) which causes the domination of NO in the spectra of the instrument background. While the NO is removed from the ionizer volume very quickly, the water background decreases only slowly since the water molecules stick more efficiently to the ionizer walls. Due to the very quick changes in the intensities of the major nitrate-related ion signals when switching on or off the aerosol load, the measured nitrate concentrations, calculated from the *difference* spectra, do not depend significantly on the length of the *beam open* and *beam closed* cycles.

The observation of increased m/z 30 to m/z 46 ratios made for less volatile nitrates (e.g. for KNO_3 we observed a ratio of ~ 28) is completely in line with this picture of the processes on the vaporizer. Since KNO_3 has lower volatility (i.e. higher melting point) compared to NH_4NO_3 the thermal decomposition progresses further for this species before ionization.

Also for ammonium sulfate the temporal behavior of the measured concentrations were determined for the individual ions with extended *beam open* and *beam closed* cycle lengths (Fig. 3b). Large differences in the temporal behavior of the signals at m/z 98 (fragment only from H_2SO_4) and m/z 80, 81 (from H_2SO_4 and SO_3) compared to the signals at m/z 48 and 64 (from H_2SO_4 and SO_3 but also from SO_2) can be seen. During the first 10 s of aerosol beam blocking the m/z 48 and 64 signals decrease to ~ 40 % of their initial value; at the end of the 17 min background measurement both

AMTD
8, 3525–3570, 2015

signals decreased down to ∼ 4 %. For the signals at m/z 80, 81, and 98 after 10 s of background measurements the signals are at 2 % for m/z 80 and at 0.3 % for m/z 81 and 98. For m/z 80 a further decrease down to 0.1 % occurs within the following 17 min. A similar behavior is found for the signal increase after restart of the aerosol measurement: for m/z 48 and 64 only ∼ 50 % of the total increase in signal occurs within the first 10 s while for m/z 80, 81, and 98 within the first 10 s already 90 (m/z 80) and more than 95 % of the final signals are recovered.

These measurements again reflect the very quick thermal decomposition (and vaporization) of ammonium sulfate into ammonia and sulfuric acid (R4). Only a very small fraction of the sulfuric acid is actually ionized before further decomposition into SO_3 (R5), which also quickly decomposes into SO_2 (R6) as indicated by the relative signal intensities and the different temporal behavior of the related ions (Fig. 3b). The slower decay of the m/z 48 and 64 signals suggests that the SO_2 molecules, which are the end products of the thermal decomposition Reactions (R4) to (R6), stick relatively efficiently to the ionizer walls. Since these two ions contain the dominating fraction of the total sulfate signal, we performed measurements to test whether this slow decay (in relation to the typical *beam open*/*beam closed* cycle lengths) of the signal causes a dependency of the measured sulfate mass concentration (calculated from the *difference* signal) on the length of the measurement cycles (0.5–20 s per half-cycle). Compared to the shortest cycle length the signal increased by 5 % when increasing the cycle length up to the maximum value. About 50 % of this increase occurs within the range of cycle lengths from 0.5 up to 5 s. Therefore for typical ranges of measurement cycle lengths only a change of sulfate measurement efficiency in the order of a few percent must be expected. However, in particle size distribution measurements or single particle measurements (e.g. for calibration purposes) the time difference between particle signal and instrument background measurement is in the order of a few milliseconds (Canagaratna et al., 2007). Here, a significant reduction in the measured sulfate concentration can be expected compared to a parallel mass concentration measurement

AMTD
8, 3525–3570, 2015

(few seconds cycle lengths), which is typically accounted for by scaling the size distribution (PTOF mode) data with mass concentration (MS mode) data.

3.3 Vaporization kinetics of semi-refractory species

The standard AMS target species are sulfate, nitrate, ammonium, chloride and organics. Water also contributes to the AMS mass spectra, however it is typically not quantified due to multiple interferences. Nevertheless, several other species or elements have been observed in measurements performed e.g. in marine air (Zorn et al., 2008; Ovadnevaite et al., 2012; Schmale et al., 2013), urban air (Salcedo et al., 2010, 2012) or of emissions from pyrotechnical devices (Drewnick et al., 2006; Faber et al., 2013). From our experience, a substance can typically be measured in the AMS with some efficiency if its melting point is not far above the vaporizer temperature. From comparison of melting point data (Haynes et al., 2015) with the typical AMS vaporizer temperature (550–600 °C) one can identify a number of metals (mainly the alkali metals) that can be expected to be measurable quite well with the AMS in their elemental state (Cd, Cs, Hg, K, Li, Na, Rb). Several others (Al, Bi, In, Mn, Pb, Te, Tl, Sn, Zn) are expected to vaporize rather slowly, but still sufficiently fast for detection with the AMS. For some of these metals their halides probably are harder to vaporize than the pure metals (Cd, Cs, K, Li, Na, Rb) while for others the halides probably vaporize more easily (Al, Bi, In, Pb, Sn, Te, Tl, Zn). Many metals can only be expected to be measurable in form of their halides (Ag, Au, Be, Co, Cr, Cu, Fe, Mo, Os, Pd, Pt, Re, Ru, Si, Sr, Ta, Ti, V, W, Zr) and not as pure metals. Most of the metal oxides have very high melting points and probably cannot be measured with the AMS while some others of these substances vaporize (Cs, Hg, Os, Ru, Se, Tl) or decompose (Ag, K, Pt, Rb, Re) at sufficiently low temperatures that they might be measurable with this instrument. The nitrates of most metals are likely measurable with the AMS due to their low melting points (alkali and alkaline earth metals, Ag, Cd, Cu, Pb) or because they decompose at sufficiently low temperature (Al, Cr, Co, Fe, Hg, Mg, Mn, Ni, Zn). Contrary, the sulfates of the alkali and alkaline earth metals and of Al, Cd, Ni and Pb are likely not measurable with the

AMTD
8, 3525–3570, 2015

AMS while those of some other metals (Ag, Cr, Co, Cu, Mn, Sn, Zn) can probably be measured with some efficiency. An overview of substances that can be expected to be measurable with the AMS based on their melting or thermal decomposition points is given in Table 1.

We have performed a number of laboratory studies focused on the detection of semi-refractory aerosol components, all being metal halides. In Fig. 4a the temporal development of the signal intensity over 25 min of continuous aerosol beam measurement followed by 25 min of instrument background measurement (three repetitions of this cycle) is shown for three ions from the ZnI_2 mass spectrum: m/z 64 (Zn^+), m/z 127 (I^+), and m/z 318 (ZnI_2^+). Apparently ZnI_2 quickly vaporizes from the AMS vaporizer resulting in an instantaneous increase and decrease of the m/z 318 signal when the particle beam is opened and blocked. Within the first 10 s after blocking the beam, the signal decreases to 0.002 % of its initial value. A quick increase to 80 % of its final value after re-opening the beam is observed within the first 10 s, however with an increase of another 20 % over the following 25 min. The m/z 64 (Zn^+) signal reacts significantly slower to changes in the aerosol flow towards the vaporizer, especially when the particle beam is blocked: after 10 s still 25 % of the initial signal level is measured, decreasing to 4 % within the following 25 min. After re-opening the aerosol beam 75 % of the signal is re-established within 10 s, further increasing over the following 25 min. The I^+-related signal (m/z 127) reacts even slower to changes in the aerosol load. Ten seconds after blocking the particle beam still 92 % of the signal remains in the mass spectra and after re-opening the beam only 10 % of the final signal is re-established after 10 s. Even during 25 min of background measurement the m/z 64 signal does not drop below 33 % of the value during the aerosol measurement. Apparently, the ZnI_2 quickly vaporizes off the vaporizer, with a large fraction of the molecules thermally decomposing. The resulting iodine and zinc efficiently stick to the ionizer walls where they slowly desorb, causing an increased background signal over extended time intervals. Therefore, for this compound no particle size distribution measurements (where variations of the signal in the range of milliseconds are measured) are possible. For iodine

AMTD
8, 3525–3570, 2015

the sticking efficiency is so large that even weeks after such a measurement significant background signal levels are observed (Drewnick et al., 2009) which can be decreased slightly faster by heating the vaporizer to an elevated temperature for several days.

When increasing the measurement half-cycle lengths from 0.5 to 30 s the mass concentrations as calculated from the *difference* signal increase by 50 % for the m/z 64 (Zn^+) and by 80 % for the m/z 127 (I^+) signal showing that variations in measurement cycle length will have a significant effect on the measured mass concentrations.

Results from similar measurements of NaCl are presented in Fig. 4b. For this aerosol component slow vaporization off and accumulation on the vaporizer is observed. During the 30 min aerosol beam measurement time no stationary state is reached for the vaporization and during the 30 min background measurement a continuous decay of the $NaCl^+$ signal is observed down to 20 % of the initial signal intensity. Within the first 10 s after blocking the aerosol beam the signal decreases by 50 % and after reopening the particle beam the signal increases to 40 % of its final level within the same time interval. This slow vaporization of NaCl from the vaporizer makes particle size distribution measurements impossible. When measuring mass concentrations, the length of the measurement cycle has an important influence on the calculated mass concentrations: they increase by 22 % when increasing the measurement half-cycle lengths from 0.5 to 30 s.

As shown in Fig. 4c increasing the vaporizer temperature from the standard value (600 °C) to higher temperatures has a strong effect on the kinetics of particle vaporization: the signal increase when opening the particle beam reflects quicker vaporization of the NaCl. At 660 °C the increase is leveling off much faster during the 30 min of measurement time; at 720 °C a plateau – i.e. a steady state in particle vaporization – is reached after about 8 min of particle measurement. In addition, even though the aerosol load was kept constant over the whole measurement, the signal intensity is increasing with increasing vaporizer temperature. The total amount of measured $NaCl^+$ ions (integrated signal intensity over whole aerosol measurement interval) increases by 75 and 230 % when increasing the vaporizer temperature from 600 to 660 and

AMTD
8, 3525–3570, 2015

720 °C, respectively. At the same time, the more efficient vaporization at elevated vaporizer temperature goes along with a reduced efficiency of ionizer self-cleaning: while at 600 °C vaporizer temperature the signal falls to 45 % of its initial value within 10 s of particle beam blocking, this decrease is only to 65 and 75 % at 660 and 720 °C, respectively. A potential reason for this slower self-cleaning of the ionizer could be that at elevated vaporizer temperatures an increased fraction of the NaCl can also desorb from the ionizer walls which at lower temperatures only act as a sink. Shift of vapor origin would result in longer time constants of NaCl removal due to the lower temperature of the ionizer wall, compared to the vaporizer. In summary, at increasing vaporizer temperature not only the aerosol signal increases but, as a consequence of the slower self-cleaning of the ionizer, also the *beam closed* signal increases. Apparently the increase in *beam closed* signal dominates over the increase in measured $NaCl^+$ ions during the *beam open* phase which results in an overall reduction of the measured NaCl mass concentration (i.e. *difference* signal) in agreement with the observations of Ovadnevaite et al. (2012).

When aerosol components slowly vaporize or efficiently stick to the ionizer walls and are slowly removed from the ionizer, large instrument background concentrations are the consequence (e.g. Salcedo et al., 2010). The ratio of the signal intensity during the background measurement (*beam closed*) to the intensity observed when the aerosol beam is measured (*beam open*), the so-called *closed-to-open ratio* (c/o), can therefore be used as a proxy for the rapidity a certain species vaporizes off the AMS vaporizer and is removed from the ionizer volume. For non-refractory species like ammonium nitrate c/o is typically in the order of 1 % or even less. Very slowly vaporizing substances have c/o ratios approaching 100 %. In a further set of measurements c/o was determined during measurements of various semi-refractory components. In Fig. 5 c/o is presented for the first 30 min of measurements of $FeCl_3 \cdot 6H_2O$ (Fig. 5a) and for the first 14 min of measurements of $SrCl_2 \cdot 6H_2O$ (Fig. 5b). In these experiments the AMS was operated with a vaporizer temperature of 600 °C and a measurement half-cycle length of 7.5 s (*beam open* and *beam closed*, each).

AMTD
8, 3525–3570, 2015

Ions resulting from the measurement of iron chloride show very different vaporization behavior (Fig. 5a). The $FeClNH_3^+$ signal (probably from partial formation of $FeCl_3NH_3$ in the particles by reaction with ammonia in the inlet line) has a c/o close to zero, which indicates that this fragment vaporizes very quickly and does not accumulate in the ionizer volume, similarly to $FeCl_3^+$, which has a c/o of 2 %. A large degree of accumulation in the ionizer volume builds up during the first 10 min of measurement for the ions Fe^+, $FeCl^+$ and $FeCl_2^+$. This results in c/o ratios of ~ 32 % for $FeCl_2^+$ and ~ 26 % for the other two ions, likely as a consequence of slow removal from the ionizer volume because the related molecules stick efficiently at the ionizer walls. The difference in behavior for these ions suggests that $FeCl_3$ vaporizes quickly but thermally decomposes into $FeCl_2$ which sticks sufficiently well to the ionizer walls to cause accumulation in the ionizer volume.

The Sr^+ and $SrCl^+$ ions from the measurement of strontium chloride both show similar vaporization behavior (Fig. 5b). Two minutes after the beginning of the measurement, c/o ratios in the order of 100 % are reached. Apparently $SrCl_2$ vaporizes very slowly off the vaporizer, resulting in very little difference between the signals during aerosol measurement and background measurement.

In order to obtain quantitative information on aerosol mass concentrations for semi-refractory aerosol components not only the relative efficiency to ionize the evolved vapor molecules (relative ionization efficiency, RIE) but also the effect of slow vaporization and slow removal from the vaporizer volume and consequently high background (*beam closed*) signals has to be taken into account. For this purpose we extend the concept of RIE also onto the latter effect. These extended RIE values can be determined in two ways. (1) By comparison of the calculated mass concentration of a test aerosol of pure particles with known particle sizes and number concentrations with its nitrate equivalent mass concentration (the measured mass concentration using RIE = 1), named RIE_{pure}. (2) By comparison of the measured nitrate equivalent mass concentration of the species with the measured mass concentration of a second species which is internally mixed in the test aerosol at a known ratio, named RIE_{mix}. Generally, any RIE value

AMTD
8, 3525–3570, 2015

obtained for semi-refractory components is valid only for the *beam open*/*beam closed* cycle length and for the vaporizer temperature for which it was determined. The major difference between the two approaches to determine RIE is that RIE_{pure} inherently contains the efficiency of particle collection on the vaporizer (collection efficiency, CE), while RIE_{mix} does not contain CE. Under the assumption that CE is not different for the pure and the mixed particle, the ratio of RIE_{mix}/RIE_{pure} provides the CE value for the respective type of particle. In Table 2 RIE_{pure}, RIE_{mix}, and calculated CE values are provided for a number of semi-refractory species which were investigated in laboratory experiments. In addition the measured c/o ratios for these species are provided.

As expected, the measured RIE values for the semi-refractory species are well below unity. Especially for species with large c/o ratios ($SrCl_2 \cdot 6\,H_2O$, $BaCl_2 \cdot 2\,H_2O$) very large corrections of the measured mass concentrations are needed to obtain the correct aerosol concentration. All CE values determined from the ratio of the two types of RIE are very low (0.03–0.11), with the exception of the CE value for KCl, which is unrealistically high (1.75). This result shows that the assumption that CE is the same for the pure and the mixed particles is not generally realistic, which was already shown for internally mixed ammonium nitrate and ammonium sulfate particles (Matthew et al., 2008; Middlebrook et al., 2012). Therefore both types of RIE values provide only information on the magnitude of the correction factor needed to obtain realistic aerosol mass concentrations for these semi-refractory species, and how they are related to their c/o ratios. Furthermore, repeated measurements of RIE for $FeCl_3 \cdot 6\,H_2O$ over one year with multiple other laboratory and field measurements in between have shown that the obtained RIE values (especially RIE_{mix}) are subject to significant changes and apparently depend on the history of the vaporizer (i.e. the "conditioning" by previously measured aerosols). In these measurements an average RIE_{pure} of 0.0061 ± 0.0025 and RIE_{mix} of 0.064 ± 0.083 were determined. Finally, several experiments have provided evidence for matrix effects where as a consequence of chemical reactions of the semi-refractory aerosol component with a matrix component (e.g. ammonium) significant changes in vaporization kinetics (i.e. in c/o ratios) are observed, which in turn result in changes in

AMTD
8, 3525–3570, 2015

RIE. Taking this into account, RIE values for semi-refractory components determined from internal mixtures with other species (RIE_{mix}) should not be generalized for mixtures with different components without further investigation of these effects.

4 Chemical reactions on the vaporizer

The purpose of the vaporizer is to transfer heat to the particles and to induce quick vaporization of the aerosol components. Other interactions between the vaporizer and the particle components like the initiation of chemical reactions between aerosol components or even chemical reactions between aerosol components and the vaporizer are not desired. Nevertheless, such reactions occur during aerosol measurements. In the standard AMS analysis procedure (Allan et al., 2004b) particulate chloride is always determined from the signal at m/z 35 ($^{35}Cl^+$) and 37 ($^{37}Cl^+$) but also at m/z 36 ($H^{35}Cl^+$) and 38 ($H^{37}Cl^+$). For NH_4Cl the latter ions can be the result of the thermal decomposition process ($NH_4Cl \rightleftharpoons NH_3 + HCl$), but since these ions are also observed for other Cl-containing species investigated here (e.g. NaCl or KCl), they are probably also the result of heat-induced chemical reactions of the chlorine with water during the vaporization process. In several measurements, both in the laboratory but also in the field, we found evidence for chemical reactions on the vaporizer. Here we present a summary of such findings associated with reactions between aerosol (i.e. particle and carrier gas) components and between aerosol components and the vaporizer.

4.1 Effects of oxygen in the carrier gas

In order to investigate potential chemical reactions of oxygen from the carrier gas with particle components during the measurement with the AMS, experiments have been performed where the same test aerosol, dispersed alternately in air and in argon, has been measured. For this purpose the atomizer and the dilution and conditioning chamber (Fig. 1) have been operated with argon (> 99.996 %) or dry air (1.5 % RH) until the

AMTD
8, 3525–3570, 2015

respective signals in the mass spectra stabilized before the actual aerosol measurement. In these experiments for ammonium nitrate and ammonium sulfate no differences have been observed in the mass spectra with the two different carrier gases.

The degree of oxidation of organic aerosol components is an important information about the age of an aerosol and its degree of atmospheric processing (Jimenez et al., 2009). For this purpose the ratio of oxygen to carbon (O/C ratio) is frequently determined in aerosol analysis. Applying high-resolution elemental analysis to AMS mass spectra of organic aerosols O/C ratios can be determined with a precision of 5 % (Aiken et al., 2007). In order to test whether O/C ratios measured with the AMS are biased by oxidation of aerosol material during the vaporization process, experiments have been performed where aerosol particles consisting of non-oxygen containing hydrocarbons (n-hexane, n-decane, polystyrene latex – PSL, and isopropylbenzene) have been measured with the AMS, alternately with air and argon as carrier gases and alternately with and without aerosol particles in the carrier gas flow. For measurements with and without the aerosol particles the aerosol was passed through a DMA which was used as a switch for the particles without changing any of the other measurement conditions (Fig. 1).

With the exception of CO_2^+ (m/z 44) no oxygen-containing ions were found in the mass spectra of all four species. Since CO_2^+ is an ion that is also obtained from the air which is analyzed together with the aerosol particles, special care has been taken to separate this "*airbeam*"-related CO_2^+ from the particle-related CO_2^+. This was done by calculating the difference of mass spectra with and without aerosol particles (under otherwise unchanged conditions) and by inspecting the PTOF spectra (see Canagaratna et al., 2007) which allow a separation of signal from the *airbeam* and from the particles.

Using air as a carrier gas, when switching on the aerosol an increase in measured CO_2^+ signal of 14 and 29 % was observed for the aliphatic hydrocarbons n-hexane (C_6H_{14}) and n-decane ($C_{10}H_{22}$), respectively. This translates into a fraction of 0.09 % (for n-hexane) and 0.16 % (for n-decane) of the total measured organics concentration. Since the m/z 44 signal is used to calculate organics-related contributions to m/z 16,

AMTD
8, 3525–3570, 2015

17, 18, and 28 (Allan et al., 2004b; Aiken et al., 2008) the overall contribution of this particle-related CO_2^+ signal to the total organics concentration is 0.2 % (n-hexane) and 0.4 % (n-decane). This results in a measured O/C ratio of 0.0016 and 0.003 for n-hexane and n-decane, respectively. Measurements with argon as carrier gas did not provide clear results since it was not possible to quantitatively replace the air in the carrier gas of the measured aerosol. Additional measurements in the PTOF mode which provide information on the size distribution of the particles clearly showed that for both hydrocarbons the change in CO_2^+ signals was associated with particle-related CO_2^+.

Two aromatic hydrocarbons, i.e. polystyrene latex (PSL, $(C_8H_8)_n$) and isopropyl-benzene (C_9H_{12}), have also been tested for potential oxidation during measurement in the AMS. For PSL an increase in CO_2^+ signal by 55 % compared to the value obtained when measuring particle-free air was observed; for isopropyl-benzene an increase of 170 % was found. For PSL this translates into 0.8 % contribution to the total organics signal which results in a measured O/C ratio of 0.005; for isopropyl-benzene the increase of total organics signal is 2.2 % and consequently the measured O/C ratio is 0.018. Also for these species PTOF measurements have shown that the observed increase in CO_2^+ ion signal is associated with the aerosol particles. This increase is significantly reduced when argon was used as a carrier gas instead of air. In summary these measurements have shown that organic species can be partially oxidized by oxygen from the remaining carrier gas when the particles are vaporized in the AMS, resulting in increased O/C ratios.

4.2 Effects of carrier gas humidity

To investigate potential reactions of the vaporizing particle material with water vapor from the carrier gas (air), experiments with 1.5 and 85 % relative humidity of the aerosol have been performed by mixing the aerosol from the atomizer with particle free dilution air of known humidity (Fig. 1). For better reproducibility, before measurements at high RH the whole system has been equilibrated with particle-free high-RH air for at least 3 h and before measurements at low RH the equilibration time was at least 14 h.

AMTD
8, 3525–3570, 2015

Several alternate measurements at low and high aerosol RH were performed with all other measurement conditions unchanged and differences between the average mass spectra for both RH levels were determined.

For ammonium nitrate a slight increase in relative signal intensity of m/z 46 (NO_2^+) and m/z 63 (HNO_3^+) compared to the base peak at m/z 30 (NO^+) was observed when increasing the aerosol RH from 1.5 to 85 %. The signal at m/z 46 increases by (5.6 ± 10.5) % (average and SD) while the increase of m/z 63 signal is (13 ± 12) %, thus the changes are barely significant. The tendency of increased m/z 46 and 63 signals with increasing aerosol RH could be explained by a shift of the equilibrium of Reaction (R2) towards the reactants due to increased abundance of H_2O in the reaction zone.

For ammonium sulfate no significant changes of relative signal intensities (related to the intensity at m/z 64) were found when the aerosol RH was increased from 1.5 to 85 %; for the various ions, average changes of relative signal intensities ranged from −4 up to +3 % with an average uncertainty of ±19 %. However, when correlating the relative signal intensity with the H_2O ionizer background signal (*beam closed* m/z 18, H_2O^+) a significant increase in m/z 80, 81, and 98 signal intensity with increasing water instrument background level was found. From linear regression of the data an increase of (+38 ± 18) % was found for the m/z 80 signal, of (+27 ± 16) % for m/z 81, and of (+28 ± 17) % for m/z 98 over the range of water vapor background concentrations measured within this experiment. These results suggest that at elevated water vapor concentrations in the ionizer the equilibrium of Reaction (R5) is shifted towards the reactants, resulting in higher sulfuric acid abundance in the ionizer and consequently higher relative signal intensity of the related signals in the mass spectra.

Experiments with NaCl particles did not show any dependence of the relative intensities of the signals in the associated mass spectra from carrier gas RH; however, the absolute signal intensity increased four-fold when increasing RH from 1.5 to 85 %, likely due to an increase in collection efficiency on the vaporizer, similar to what has been observed for ammonium sulfate (Allan et al., 2004a; Matthew et al., 2008).

AMTD
8, 3525–3570, 2015

4.3 Chemical reactions with the vaporizer

A one-minute average unit-resolution mass spectrum of the aerosol in the exhaust stack of a municipal waste incinerator measured with a HR-ToF-AMS is shown in Fig. 6a. Besides the typical signals from ammonium, sulfate, nitrate and chloride also a large number of nominally organics-related signals (green) were found in the spectrum. Since in this aerosol no organic material was expected because of the complete combustion, and due to the unusual patterns of these signals the high-resolution mass spectrum was inspected in more detail. It turned out that the intense "organics-related" signals in this mass spectrum were associated with bromine, iodine and with halides of potassium, sodium, iron, nickel, zinc and lead. In addition, many intense signals above m/z 180 could be identified as $WO_2Cl_2^+$ and the various isotopes of the fragments of this ion (Fig. 6b, Table 3).

Laboratory experiments with various metal chlorides ($AlCl_3$, $BaCl_2$, $CuCl_2$, $FeCl_2$, $FeCl_3$, KCl, NaCl, $SrCl_2$) and with NH_4Cl showed that the occurrence of WO_2Cl_2 signals in the mass spectra is a general feature when measuring Cl-containing aerosol species. Apparently WO_2Cl_2 is a result of the reaction of Cl from the particles with the vaporizer surface, likely with WO_3 that is generated by oxidation of the hot tungsten vaporizer surface by oxygen from the aerosol carrier gas.

Strong indications for this process are provided by experiments where the carrier gas was switched between air and argon. Alternate measurements with both types of carrier gases resulted in WO_2Cl_2-related signals about 25 % lower in the measurements with argon, compared to those with air as carrier gas. In addition, over the course of three argon-air-cycles the WO_2Cl_2-related signals decreased more and more. Apparently the WO_3 reservoir at the vaporizer surface got more and more depleted during these measurements. Generally, with increasing Cl-concentration in the measured aerosol also the intensities of the WO_2Cl_2-related signals increase. Also for higher vaporizer temperature an increased WO_2Cl_2 signal was observed: in measurements of $FeCl_3$ aerosol the WO_2Cl_2-related signal, normalized on the Cl signal, increased by

AMTD
8, 3525–3570, 2015

a factor of two when the vaporizer temperature was increased from 600 to 800 °C. At the same time enhanced fragmentation of the WO_2Cl_2 into preferentially smaller fragments was observed in the measurements at elevated vaporizer temperature. This dependence of WO_2Cl_2 abundance from vaporizer temperature and Cl-concentration is in agreement with observations of high-temperature corrosion in industrial systems (Lai, 2007).

Time-resolved data of WO_2Cl_2 from extended aerosol *beam open/beam closed* measurements of NaCl (Fig. 4b and c) provide indications that during the background measurements tungsten from the vaporizer is oxidized which results in an accumulation of WO_3 at the vaporizer surface. When switching to the aerosol beam measurement, the reaction of the aerosol with the conditioned vaporizer surface causes a spike in measured WO_2Cl_2 signals, which lasts for about one minute (Fig. 4b). In the following minutes the WO_2Cl_2 signal increases slowly. When argon is used as a carrier gas or at higher vaporizer temperature (Fig. 4c), this WO_2Cl_2 spike at the beginning of NaCl measurements is less pronounced; apparently under these conditions the conditioning of the vaporizer during the background measurement is less efficient. Finally, the generation of WO_2Cl_2 per amount of Cl in the aerosol depends on the type of aerosol measured; in our experiments we found WO_2Cl_2 yields in the order $KCl > CuCl_2 > FeCl_3 \approx FeCl_2 > SrCl_2 > NaCl > BaCl_2 \approx AlCl_3 \approx NH_4Cl$. For KCl 12 ng m^{-3} NO_3-eq. WO_2Cl_2 was measured per µg Cl m^{-3} expected from the aerosol concentration; this yield was about 70 times larger than that for NH_4Cl (0.17 ng m^{-3} NO_3-eq./µg Cl m^{-3}). With a WO_2Cl_2 yield of 0.40 ng m^{-3} NO_3-eq./µg Cl m^{-3} NaCl ranges at the lower end of observed values. The uncertainties of these yields are approximately 15 %.

Experiments with iron salt aerosols have provided further evidence for chemical reactions at and with the vaporizer surface. As presented above, the RIE (i.e. the efficiency of quick vaporization of a substance) of $FeCl_3$ particles is affected by the vaporizer history, likely by the resulting surface properties of the vaporizer. In measurements of $FeSO_4 \cdot 7H_2O$ no iron-containing signals have been observed, both at 600 and 800 °C vaporizer temperature. The fact that intense sulfate-related signals were found in the

AMTD
8, 3525–3570, 2015

mass spectra suggests that $FeSO_4$ quickly thermally decomposes at the vaporizer surface. Likely Fe is oxidized into Fe_2O_3, which as refractory component remains on the vaporizer surface. The formation of refractory components on the vaporizer surface is problematic because these processes result in a conditioning of the vaporizer with potential effects on the vaporizer/particle interaction. Exactly this kind of effect was observed in measurements of $Fe(NO_3)_3 \cdot 9\,H_2O$ particles with the AMS: besides intense nitrate-related signals also clear ion signals of $FeCl^+$ (m/z 91, 93) and $FeCl_2^+$ (m/z 126, 128, 130) were observed in the mass spectra. After careful inspection of the whole measurement system and the particle composition the possibility of contamination of the particles with chlorine can be excluded. Therefore we assume that these ions are the result of chemical reactions between the particle material and chlorine that was bound to the vaporizer as a consequence of previous experiments with Cl-containing particles. This constitutes a veritable memory effect of the AMS vaporizer.

A different type of particle/vaporizer interaction can be observed for potassium-containing particles: due to the low ionization potential of potassium ($E_K = 4.34$ eV) these atoms can be ionized at the hot tungsten surface (work function $E_W = 4.32$ to 5.22 eV, Haynes, 2015) by surface ionization. Generally, surface ionization is not desired in AMS measurements due to the very intense signals which can be generated by this process and which are not well quantifiable (Allan et al., 2003). In equilibrium, the ratio of the number of potassium ions (n_+) to the number of potassium atoms (n_a) vaporizing from a tungsten surface is a function of the surface temperature T, the work function of tungsten, and the ionization potential of potassium and is described by the Saha–Langmuir equation (Datz and Taylor, 1956),

$$\frac{n_+}{n_a} = \frac{1 - r_+}{1 - r_a} \cdot \frac{1}{2} \cdot \exp\left[\frac{E_W - E_K}{kT}\right], \quad (1)$$

with r_+ and r_a the reflection coefficients for the ion and the atom, respectively. In the AMS KCl generates the following ions (plus isotopes): Cl^+ (m/z 35), HCl^+ (m/z 36), K^+ (m/z 39), Cl_2^+ (m/z 70), KCl^+ (m/z 74), and K_2Cl^+ (m/z 113). Since the ions

AMTD
8, 3525–3570, 2015

from surface ionization are generated at a different location than the ions from electron ionization they need to follow a different trajectory into the mass spectrometer. In addition to differences in transmission efficiency, this also causes distorted ion peaks in the mass spectra which are shifted to slightly higher m/z (Fig. 7b). Such peak distortions are observed for K^+ but not for KCl^+ and K_2Cl^+ (Fig. 7c). This shows that two different processes occur on the vaporizer: KCl partially vaporizes and in a second step this vapor is ionized by electron impact only; additionally, K atoms occurring at the vaporizer surface can undergo surface ionization with an efficiency depending on the temperature and the work function of the vaporizer.

Experiments to investigate the surface ionization process support the above-mentioned picture. Measurements of KCl aerosol at different vaporizer temperatures with and without electron impact ionization (filament turned on and off) were performed. When the filament was turned off, at 400 °C vaporizer temperature no K^+ signal was observed, i.e. no surface ionization occurred. At 600 °C vaporizer temperature strong K^+ ion signals from surface ionization were found, however, when switching on the filament the K^+ signal increased by a factor of four, indicating that at this temperature the majority of the K^+ signal stems from electron impact ionization. Finally, at even higher vaporizer temperature (800 °C) the vast majority of the K^+ signal originated from surface ionization. Measurements at this vaporizer temperature have shown that apparently a large fraction of the ions generated by surface ionization get lost on their way to the mass spectrometer when the filament is on. This is likely due to associated changes of the electric field in the ionizer volume when the filament is turned on and off. This electric field is optimized for detection of ions generated by electron impact ionization at a different location of the ionizer compared to the location where the surface ionization takes place, i.e. the vaporizer surface. Therefore the fraction of ions from surface ionization measured in these experiments is likely below the actually generated fraction of ions. The fact that in all measurements without electron impact ionization no signals from KCl^+ and K_2Cl^+ were observed supports the assumption of the above-mentioned separation of vaporization and surface ionization.

AMTD
8, 3525–3570, 2015

During the first measurements on a measurement day K^+ ions almost exclusively from electron impact ionization with the regular ion peak shape (Fig. 7a) have been observed in the high resolution mass spectra. After the measurement of several semi-refractory metal chlorides ($FeCl_3$, $BaCl_2$, $SrCl_2$, $CuCl_2$) over the day the measurements with KCl were repeated. While in these measurements no significant changes for the intensity of KCl^+ and K_2Cl^+ (both ions only from electron impact ionization) was found, the K^+ signals were more than ten times larger compared to the measurement in the morning. The observed increase in relative signal intensity and the changed ion signal peak shape (Fig. 7b) indicate that in these measurements a large fraction of the K^+ signal is from surface ionization. This change over the course of the day suggests that the vaporizer history has an important influence on the efficiency of surface ionization. Apparently the adsorption of chlorine atoms at the vaporizer surface over the day caused an increase in work function for the tungsten surface (Datz and Taylor, 1956), associated with an increase in surface ionization efficiency.

5 Discussion

Our experiments, in agreement with several previous publications (e.g. Drewnick et al., 2006; Zorn et al., 2008; Salcedo et al., 2010 and 2012; Ovadnevaite et al., 2012; Faber et al., 2013) have shown that for measurements with the AMS a sharp separation of species into non-refractory and refractory aerosol components is not valid. The standard AMS species (ammonium nitrate, ammonium sulfate, organics) vaporize very quickly from the AMS vaporizer. However, even for these species differences in vaporization event lengths were observed which can result in different efficiencies of ion transport into the ToF-MS if the extraction pulser of the mass spectrometer is not operated at sufficiently high frequency.

Beyond these standard species several other metals, many metal halides, nitrates and sulfates, as well as a few metal oxides can be measured or can be expected to be measurable with the AMS with some efficiency. From our experience, the melting

AMTD
8, 3525–3570, 2015

point of a species can serve as a rough indicator: if it is not well above the vaporizer temperature one can expect that the substance can be measured with the AMS. Due to slow vaporization from the vaporizer or efficient adsorption/desorption at the slightly colder ionizer walls vaporization event lengths for such species can be dramatically extended, from a few tens of microseconds for non-refractory species up to minutes or even more for semi-refractory species. Under such conditions no particle size distribution measurements are possible with the AMS. In addition, such slow vaporization results in a significant fraction of the particle material to vaporize when nominally the instrument background is measured. This increases the *beam closed*/*beam open* ratio (c/o) and as a consequence reduces the *difference* signal which is used for calculation of particle mass concentrations. In order to obtain quantitative mass concentrations for such species relative ionization efficiencies (RIE) which include the effect of slow vaporization must be determined for each species. While the AMS is generally capable of providing some information on the abundance of such species, quantification with RIE values is possible only to a very limited degree. An RIE value determined for a certain semi-refractory species in the laboratory is only valid for the applied vaporizer temperature and measurement cycle frequency; in addition, our measurements have shown that such RIE values are also dependent on the particle matrix, i.e. the components internally mixed with the target substance, and on the vaporizer history, i.e. the previous measurements with the instrument. Also, since for a given c/o very different RIE values are observed, c/o alone seems not always to be a sufficient basis for reliable quantification of such species. As a consequence, under general conditions such semi-refractory components are only quantifiable with large uncertainties.

While in typical ambient measurements of continental or urban aerosol with the AMS the effects presented here will not measurably affect the determination of the standard AMS species concentrations, under certain conditions they can have significant effects on the obtained mass spectra: in laboratory experiments of aerosols containing semi-refractory material, in measurements close to certain anthropogenic sources or in measurements in the remote marine environment. In measurements in the exhaust

AMTD
8, 3525–3570, 2015

of municipal and hazardous waste incinerators we observed strong signals of multiple semi-refractory components like metal halides and WO_2Cl_2 from reaction of particulate Cl with the oxidized vaporizer. Most of these signals were observed at nominally organics-related m/z. Under such conditions, where essentially no organic material is in the aerosol (due to complete combustion) or where very large Cl concentrations occur, such misidentified ion signals can dominate the total mass spectrum and lead to a distorted picture of the aerosol composition. For example during measurements in the remote marine aerosol WO_2Cl_2, stemming from the very abundant sea salt, was observed, which would have caused an erroneous increase of "organics" mass concentration by 50 % if not correctly interpreted (Zorn, 2009). From the WO_2Cl_2 yields provided above one can estimate that the ambient particulate Cl concentration must be between 0.6 and 42 times the measured organics concentration in order that the WO_2Cl_2-related signals exceed the organics contribution to the mass spectrum in the upper m/z range (m/z 180–300). For NaCl particulate chlorine must be 18 times the organics mass concentration.

Especially during laboratory measurements where the exact composition of aerosol components or elemental ratios are desired the possibility of chemical reactions on or with the vaporizer should be taken into account. Experiments have shown that the AMS vaporizer does not always act as inert vehicle of energy transported to the particles. Chemical reactions of particle components with oxygen or water in the carrier gas or with components from previous experiments which were accumulated on the vaporizer can result in ion signals in the mass spectra which do not reflect components of the measured aerosol. In principle organic material can be oxidized on the vaporizer and cause positively biased O/C ratios, however, this effect seems to be very small and typically well below the uncertainty of such measurements. In our experiments O/C ratios of non-oxygen containing species were in the range of 0.0016 to 0.018. The lowest O/C ratios observed in measurements of ambient aerosol are for hydrocarbon-like organic aerosol (HOA, 0.13) and cooking-related organic aerosol (COA, 0.22) while

AMTD
8, 3525–3570, 2015

aged organic aerosol has O/C ratios ranging between 0.50 and 0.85 (Canagaratna et al., 2015).

6 Summary

Various experiments to investigate the interaction of aerosol particles with the vaporizer of the Aerodyne AMS and resulting consequences for the measured mass spectra were conducted. Overall, these investigations show that the AMS vaporizer does not always behave inertly towards the particles and that no sharp separation into non-refractory and refractory components can be made for AMS measurements.

Highly time-resolved measurements of single particle vaporization events of non-refractory aerosol components (NH_4NO_3 and $(NH_4)_2SO_4$) show that above a species-dependent vaporizer temperature threshold vaporization event lengths are in the order of 25–50 µs (FWHM) and do not depend on vaporizer temperature. For certain fragments (NO, SO_2) longer particle vaporization event lengths are observed compared to the other fragments, likely due to a combination of thermal decomposition processes and sticking probabilities to the ionizer wall surfaces. For slow ion extraction frequencies into the mass spectrometer (e.g. for the HR-ToF-AMS) these differences can cause different measurement efficiencies for the different ions.

Time-resolved measurements of aerosol and instrument background over extended time intervals provide information on vaporization kinetics for non-refractory and semi-refractory aerosol components. Very quick vaporization of NH_4NO_3 and removal from the ionizer volume cause quick changes in related ion intensities when the aerosol load changes. For $(NH_4)_2SO_4$ different behavior is found for different ions: while sulfuric acid-related ions also show quick changes in intensity, SO_2-related ion intensities adjust much slower to abrupt changes in aerosol load, likely because they are the end-products of the thermal decomposition process and can stick with some probability to the ionizer walls.

AMTD
8, 3525–3570, 2015

In order to quantify semi-refractory species relative ionization efficiencies (RIE) have been determined for a number of metal chlorides. As expected RIE values for these species are well below unity and are very small (< 0.001) for species with very large *beam closed*/*beam open* ratios. As a consequence measured signals have to be multiplied with very large factors in order to obtain ambient mass concentrations. Furthermore, experiments have shown that the RIE values for semi-refractory species do not only depend on vaporizer temperature and measurement cycle length, but can also depend on the aerosol matrix (i.e. the components which are internally mixed with the target species) and the vaporizer history (i.e. previous measurements with the same instrument which can cause conditioning of the vaporizer). Similarly, for KCl the efficiency of surface ionization of potassium was found to be strongly dependent on the vaporizer history. As a consequence of these effects, under general conditions, quantitative measurements of semi-refractory aerosol components are subject to large uncertainties.

Experiments with argon as carrier gas and with different carrier gas humidities have shown that the mass spectra of certain aerosol species are influenced by chemical reactions at the vaporizer. Slight changes in relative peak intensities of some of the fragments of NH_4NO_3 and $(NH_4)_2SO_4$ have been found when carrier gas RH changed. In measurements of non-oxygen containing aliphatic and aromatic hydrocarbons small amounts of oxidation have been observed, resulting in O/C values in the range of 0.0016 to 0.018, i.e. within the uncertainty of typical ambient O/C ratio measurements.

In addition to chemical reactions of particle and carrier gas components at the vaporizer also chemical reactions of aerosol components with the vaporizer have been observed. In measurements of Cl-containing species ions of WO_2Cl_2 and its fragments and isotopes can be observed, likely from the reaction of Cl with WO_3 on the vaporizer surface. In other measurements we observed $FeCl^+$ and $FeCl_2^+$ ions during the measurement of $Fe(NO_3)_3$, likely from Cl that was accumulated on the vaporizer during previous experiments. In measurements of $FeSO_4$ only sulfate-related signals have been observed. The iron likely reacted on the vaporizer to Fe_2O_3 which as a refractory species remains on the vaporizer. Generally, such conditioning of the vaporizer

AMTD
8, 3525–3570, 2015

material does not only generate a potential reservoir for ions in mass spectra of future measurements but can also change relative ionization and collection efficiencies.

While the effects observed in these experiments will not have a significant influence on general ambient measurements of continental or urban aerosols, they can significantly affect the mass spectra under certain conditions like in measurements of laboratory aerosols, probing of anthropogenic sources or in the measurement of remote marine aerosols.

Acknowledgements. The authors thank F. Freutel for helpful discussions.

The article processing charges for this open-access publication have been covered by the Max Planck Society.

References

Aiken, A. C., DeCarlo, P. F., and Jimenez, J. L.: Elemental analysis of organic species with electron ionization high-resolution mass spectrometry, Anal. Chem., 79, 8350–8358, 2007.

Aiken, A. C., DeCarlo, P. F., Kroll, J. H., Worsnop, D. R., Huffman, J. A., Docherty, K. S., Ulbrich, I. M., Mohr, C., Kimmel, J. R., Sueper, D., Sun, Y., Zhang, Q., Trimborn, A., Northway, M., Ziemann, P. J., Canagaratna, M. R., Onasch, T. B., Alfarra, M. R., Prevot, A. S. H., Dommen, J., Duplissy, J., Metzger, A., Baltensperger, U., and Jimenez, J. L.: O/C and OM/OC ratios of primary, secondary, and ambient organic aerosols with high-resolution time-of-flight aerosol mass spectrometry, Environ. Sci. Technol., 42, 4478–4485, 2008.

Allan, J. D., Alfarra, M. R., Bower, K. N., Williams, P. I., Gallagher, M. W., Jimenez, J. L., McDonald, A. G., Nemitz, E., Canagaratna, M. R., Jayne, J. T., Coe, H., and Worsnop, D. R.: Quantitative sampling using an aerodyne aerosol mass spectrometer, 2, measurements of fine particulate chemical composition in two UK cities, J. Geophys. Res.-Atmos., 108, 4091, doi:10.1029/2002JD002359, 2003.

Allan, J. D., Bower, K. N., Coe, H., Boudries, H., Jayne, J. T., Canagaratna, M. R., Millet, D. B., Goldstein, A. H., Quinn, P. K., Weber, R. J., and Worsnop, D. R.: Submicron aerosol composition at Trinidad Head, California, during ITCT 2K2: its relationship with gas phase volatile

AMTD
8, 3525–3570, 2015

organic carbon and assessment of instrument performance, J. Geophys. Res.-Atmos., 109, D23S24, doi:10.1029/2003JD004208, 2004a.
Allan, J. D., Delia, A. E., Coe, H., Bower, K. N., Alfarra, M. R., Jimenez, J. L., Middlebrook, A. M., Drewnick, F., Onasch, T. B., Canagaratna, M. R., Jayne, J. T., and Worsnop, D. R.: A generalized method for the extraction of chemically resolved mass spectra from aerodyne aerosol mass spectrometer data, J. Aerosol. Sci., 35, 909–922, 2004b.
Allen, J. and Gould, R. K.: Mass spectrometric analyzer for individual aerosol particles, Rev. Sci. Instrum., 52, 804–809, 1981.
Canagaratna, M. R., Jayne, J. T., Jimenez, J. L., Allan, J. D., Alfarra, M. R., Zhang, Q., Onasch, T. B., Drewnick, F., Coe, H., Middlebrook, A., Delia, A., Williams, L. R., Trimborn, A. M., Northway, M. J., DeCarlo, P. F., Kolb, C. E., Davidovits, P., and Worsnop, D. R.: Chemical and microphysical characterization of ambient aerosols with the aerodyne aerosol mass spectrometer, Mass. Spectrom. Rev., 26, 185–222, 2007.
Canagaratna, M. R., Jimenez, J. L., Kroll, J. H., Chen, Q., Kessler, S. H., Massoli, P., Hildebrandt Ruiz, L., Fortner, E., Williams, L. R., Wilson, K. R., Surratt, J. D., Donahue, N. M., Jayne, J. T., and Worsnop, D. R.: Elemental ration measurements of organic compounds using aerosol mass spectrometry: characterization, improved calibration, and implications, Atmos. Chem. Phys. 15, 253–272, doi:10.5194/acp-15-253-2015, 2015.
Chinn, J. W. and Lagow, R. J.: Characterization of the vapor species of methyllithium by flash vaporization mass spectrometry, Organometallics, 3, 75–77, 1984.
Dall'Osto, M., Drewnick, F., Fisher, R., and Harrison, R. M.: Real-time measurements of non-metallic fine particulate matter adjacent to a major integrated steelworks, Aerosol. Sci. Tech., 46, 639–653, 2012.
Davis, W. D.: Surface ionization mass spectroscopy of airborne particulates, J. Vac. Sci. Technol., 10, 278, 1973.
Datz, S. and Taylor, E. H.: Ionization on platinum and tungsten surfaces, I, the alkali metals, J. Chem. Phys., 25, 389–394, 1956.
DeCarlo, P. F., Kimmel, J. R., Trimborn, A., Northway, M. J., Jayne, J. T., Aiken, A. C., Gonin, M., Fuhrer, K., Horwarth, T., Docherty, K. S., Worsnop, D. R., and Jimenez, J. L.: Field-deployable, high-resolution, time-of-flight aerosol mass spectrometer, Anal. Chem., 78, 8281–8289, 2006.
Drewnick, F., Hings, S. S., DeCarlo, P., Jayne, J. T., Gonin, M., Fuhrer, K., Weimer, S., Jimenez, J. L., Demerjian, K. L., Borrmann, S., and Worsnop, D. R.: A new time-of-flight

AMTD
8, 3525–3570, 2015

aerosol mass spectrometer (TOF-AMS) – instrument description and first field deployment, Aerosol. Sci. Tech., 39, 637–658, 2005.
Drewnick, F., Hings, S. S., Curtius, J., Eerdekens, G., and Williams, J.: Measurement of fine particulate and gas-phase species during the New Year's fireworks 2005 in Mainz, Germany, Atmos. Environ., 40, 4316–4327, 2006.
Drewnick, F., Hings, S. S., Alfarra, M. R., Prevot, A. S. H., and Borrmann, S.: Aerosol quantification with the aerodyne aerosol mass spectrometer: detection limits and ionizer background effects, Atmos. Meas. Tech., 2, 33–46, doi:10.5194/amt-2-33-2009, 2009.
Faber, P., Drewnick, F., Veres, P. R., Williams, J., and Borrmann, S.: Anthropogenic sources of aerosol particles in a football stadium: real-time characterization of emissions from cigarette smoking, cooking, hand flares, and color smoke bombs by high-resolution aerosol mass spectrometry, Atmos. Environ., 77, 1043–1051, 2013.
Friedel, R. A., Sharkey Jr., A. G., Schultz, J. L., and Humbert, C. R.: Mass spectrometric analysis of mixtures containing nitrogen dioxide, Anal. Chem., 25, 1314–1320, 1953.
Haynes, W. M., Baysinger, G., Berger, L. I., Frenkel, M., Goldberg, R. N., Kuchitsu, K., Roth, D. L., and Zwillinger, D.: CRC Handbook of Chemistry and Physics, 95th edn., Internet Version 2015, CRC Press/Taylor and Francis, Boca Raton, FL, 2015.
Jayne, J. T., Leard, D. C., Zhang, X., Davidovits, P., Smith, K. A., Kolb, C. E., and Worsnop, D. R.: Development of an aerosol mass spectrometer for size and composition analysis of submicron particles, Aerosol. Sci. Tech., 33, 49–70, 2000.
Jimenez, J. L., Jayne, J. T., Shi, Q., Kolb, C. E., Worsnop, D. R., Yourshaw, I., Seinfeld, J. H., Flagan, R. C., Zhang, X., Smith, K. A., Morris, J. W., and Davidovits, P.: Ambient aerosol sampling using the aerodyne aerosol mass spectrometer, J. Geophys. Res.-Atmos., 108, 8425, doi:10.1029/2001JD001213, 2003.
Jimenez, J. L., Canagaratna, M. R., Donahue, N. M., Prevot, A. S. H., Zhang, Q., Kroll, J., DeCarlo, P. F., Allan, J. D., Coe, H., Ng, N. L., Aiken, A. C., Docherty, K. S., Ulbrich, I. M., Grieshop, A. P., Robinson, A. L., Duplissy, J., Smith, J. D., Wilson, K. R., Lanz, V. A., Hueglin, C., Sun, Y. L., Tian, J., Laaksonen, A., Raatikainen, T., Rautiainen, J., Vaattovaara, P., Ehn, M., Kulmala, M., Tomlinson, J. M., Collins, D. R., Cubison, M. J., Dunlea, E. J., Huffman, J. A., Onasch, T. B., Alfarra, M. R., Williams, P. I., Bower, K., Kondo, Y., Schneider, J., Drewnick, F., Borrmann, S., Weimer, S., Demerjian, K., Salcedo, D., Cottrell, L., Griffin, R., Takami, A., Miyoshi, T., Hatakeyama, S., Shimono, A., Sun, J. Y., Zhang, Y. M., Dzepina, K., Kimmel, J. R., Sueper, D., Jayne, J. T., Herndon, S. C., Trimborn, A. M.,

AMTD
8, 3525–3570, 2015

Williams, L. R., Wood, E. C., Middlebrook, A. M., Kolb, C. E., Baltensperger, U., and Worsnop, D. R.: Evolution of organic aerosols in the atmosphere, Science, 326, 1525–1529, 2009.

Lai, G. Y.: High-Temperature Corrosion and Materials Applications, ASM International, Materials Park, Ohio, USA, 2007.

de Leeuw, J. W., de Leer, E. W. B., Sinninghe Damsté, J. S., and Schuyl, P. J. W.: Screening of anthropogenic compounds in polluted sediments and soils by flash evaporation/pyrolysis gas chromatography-mass spectrometry, Anal. Chem., 58, 1852–1857, 1986.

Lim, H.-J., Turpin, B. J., Edgerton, E., Hering, S. V., Allen, G., Maring, H., and Solomon, P.: Semicontinuous aerosol carbon measurements: comparison of Atlanta Supersite measurements, J. Geophys. Res.-Atmos., 108, 8419, doi:10.1029/2001JD001214, 2003.

Lincoln, K. A.: Flash-vaporization of solid materials for mass spectrometry by intense thermal radiation, Anal. Chem., 37, 541–543, 1965.

Matthew, B. M., Middlebrook, A. M., and Onasch, T.: Collection efficiencies in an aerodyne aerosol mass spectrometer as a function of particle phase for laboratory generated aerosols, Aerosol. Sci. Tech., 42, 884–898, 2008.

Middlebrook, A. M., Bahreini, R., Jimenez, J. L., and Canagaratna, M. R.: Evaluation of composition-dependent collection efficiencies for the aerodyne aerosol mass spectrometer using field data, Aerosol. Sci. Tech., 46, 258–271, 2012.

Ovadnevaite, J., Ceburnis, D., Canagaratna, M., Berresheim, H., Bialek, J., Martucci, G., Worsnop, D. R., and O'Dowd, C.: On the effect of wind speed on submicron sea salt mass concentrations and source fluxes, J. Geophys. Res.-Atmos., 117, D1621, doi:10.1029/2011JD017379, 2012.

Roberts, P. T. and Friedlander, S. K.: Analysis of sulfur in deposited aerosol particles by vaporization and flame photometric detection, Atmos. Environ., 10, 403–408, 1976.

Salcedo, D., Onasch, T. B., Aiken, A. C., Williams, L. R., de Foy, B., Cubison, M. J., Worsnop, D. R., Molina, L. T., and Jimenez, J. L.: Determination of particulate lead using aerosol mass spectrometry: MILAGRO/MCMA-2006 observations, Atmos. Chem. Phys., 10, 5371–5389, doi:10.5194/acp-10-5371-2010, 2010.

Salcedo, D., Laskin, A., Shutthanandan, V., and Jimenez, J.-L.: Feasibility of the detection of trace elements in particulate matter using online high-resolution aerosol mass spectrometry, Aerosol. Sci. Tech., 46, 1187–1200, 2012.

AMTD
8, 3525–3570, 2015

Schmale, J., Schneider, J., Nemitz, E., Tang, Y. S., Dragosits, U., Blackall, T. D., Trathan, P. N., Phillips, G. J., Sutton, M., and Braban, C. F.: Sub-Antarctic marine aerosol: dominant contributions from biogenic sources, Atmos. Chem. Phys., 13, 8669–8694, doi:10.5194/acp-13-8669-2013, 2013.

Sinha, M. P., Giffin, C. E., Norris, D. D., Estes, T. J., Vilker, V. L., and Friedlander, S. K.: Particle analysis by mass spectrometry, J. Colloid. Interf. Sci., 87, 140–153, 1982.

Stoffels, J. J. and Lagergren, C. R.: On the real-time measurement of particles in air by direct-inlet surface ionization mass spectrometry, Int. J. Mass Spectrom., 40, 243–254, 1981.

Stolzenburg, M. R. and Hering, S. V.: Method for the automated measurement of fine particle nitrate in the atmosphere, Environ. Sci. Technol., 34, 907–914, 2000.

Stolzenburg, M. R., Dutcher, D. D., Kirby, B. W., and Hering, S. V.: Automated measurement of the size and concentration of airborne particulate nitrate, Aerosol. Sci. Tech., 37, 537–546, 2003.

Takegawa, N., Miyakawa, T., Watanabe, M., Kondo, Y., Miyazaki, Y., Han, S., Zhao, Y., van Pinxteren, D., Bruggemann, E., Gnauk, T., Herrmann, H., Xiao, R., Deng, Z., Hu, M., Zhu, T., and Zhang, Y.: Performance of an aerodyne aerosol mass spectrometer (AMS) during intensive campaigns in China in the summer of 2006, Aerosol. Sci. Tech., 43, 189–204, 2009.

Zorn, S. R.: Chemical Composition Measurements of Pristine Aerosols in the Southern Atlantic and Amazonian Regions by Means of On-line Time-of-Flight Aerosol Mass Spectrometry, Dissertation, Johannes-Gutenberg-University, Mainz, Germany, 2009.

Zorn, S. R., Drewnick, F., Schott, M.,Hoffmann, T., and Borrmann, S.: Characterization of the South Atlantic marine boundary layer aerosol using an aerodyne aerosol mass spectrometer, Atmos. Chem. Phys., 8, 4711–4728, doi:10.5194/acp-8-4711-2008, 2008.

AMTD
8, 3525–3570, 2015

Table 1. Overview of elements which can be expected to be measurable in elemental state or as halide, oxide, nitrate, or sulfate with the AMS based on their melting or thermal decomposition points.

Chemical compound class	Elements potentially measurable with AMS
elemental	Al, Bi, Cd, Cs, Hg, In, K, Li, Mn, Na, P, Rb, Te, Tl, Sn, Zn
halide	Ag, Al, Au, Be, Bi, Co, Cr, Cu, Fe, In, Mo, Os, Pb, Pd, Pt, Re, Ru, Si, Sn, Sr, Ta, Te, Ti, Tl, V, W, Zn, Zr
oxide	Ag, Cs, Hg, K, Os, Pt, Rb, Re, Ru, Se, Tl
nitrate	Ag, Al, Ba, Be, Ca, Cd, Cr, Co, Cs, Cu, Fe, Hg, K, Li, Mg, Mn, Na, Ni, Pb, Sr, Zn
sulfate	Ag, Cr, Co, Cu, Mn, Sn, Zn

AMTD
8, 3525–3570, 2015

Table 2. Relative ionization efficiencies, CE values and c/o ratios for the metals from various metal halides measured during one set of experiments. RIE values were determined with two different approaches (RIE_{pure}, RIE_{mix}). CE values are calculated from the ratio of RIE_{mix}/RIE_{pure}. The measurement uncertainty is ~ 15 % for RIE and ~ 20 % for CE values. For the determination of RIE_{mix}, most species were internally mixed with $(NH_4)_2SO_4$; only $BaCl_2$ and $SrCl_2$ were mixed with NH_4Cl.

	$FeCl_3 \cdot 6H_2O$	$AlCl_3 \cdot 6H_2O$	$CuCl_2 \cdot 2H_2O$	$SrCl_2 \cdot 6H_2O$	$BaCl_2 \cdot 2H_2O$	KCl
RIE_{pure}	0.0089	0.0009	0.0242	< 0.0001	< 0.0001	0.0017
RIE_{mix}	0.1584	0.0086	0.2317	0.0005	0.0006	0.0010
CE	0.06	0.11	0.11	0.04	0.03	1.75
c/o_{pure} (%)	12 ± 1	16 ± 3	26 ± 4	79 ± 12	98 ± 3	4 ± 1
c/o_{mix} (%)	20 ± 4	8 ± 1	19 ± 3	98 ± 1	97 ± 5	25 ± 9

AMTD
8, 3525–3570, 2015

Table 3. Fragments and isotopes (only W isotopes with > 1 % relative abundance are considered) of tungsten oxide chloride (WO_2Cl_2).

Fragment	Signal at m/z
W^+	182, 183, 184, 186
WO^+	198, 199, 200, 202
WO_2^+	214, 215, 216, 218
WCl^+	217, 218, 219, 220, 221, 223
$WOCl^+$	233, 234, 235, 236, 237, 239
WO_2Cl^+	249, 250, 251, 252, 253, 255
WCl_2^+	252, 253, 254, 255, 256, 258, 260
$WOCl_2^+$	268, 269, 270, 271, 272, 274, 276
$WO_2Cl_2^+$	284, 285, 286, 287, 288, 290, 292

AMTD
8, 3525–3570, 2015

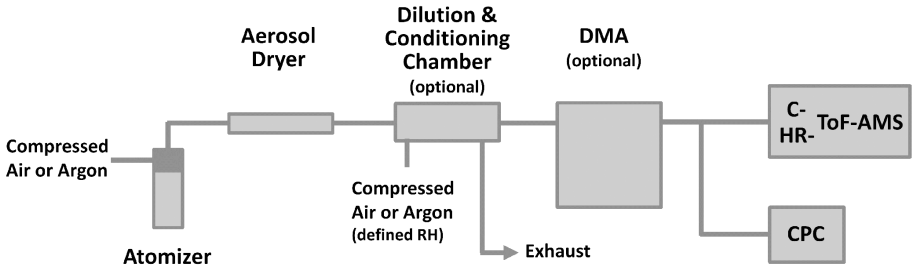

Figure 1. Setup for the measurements of non-refractory and semi-refractory aerosols with defined carrier gas humidity and with air and argon as carrier gas.

AMTD
8, 3525–3570, 2015

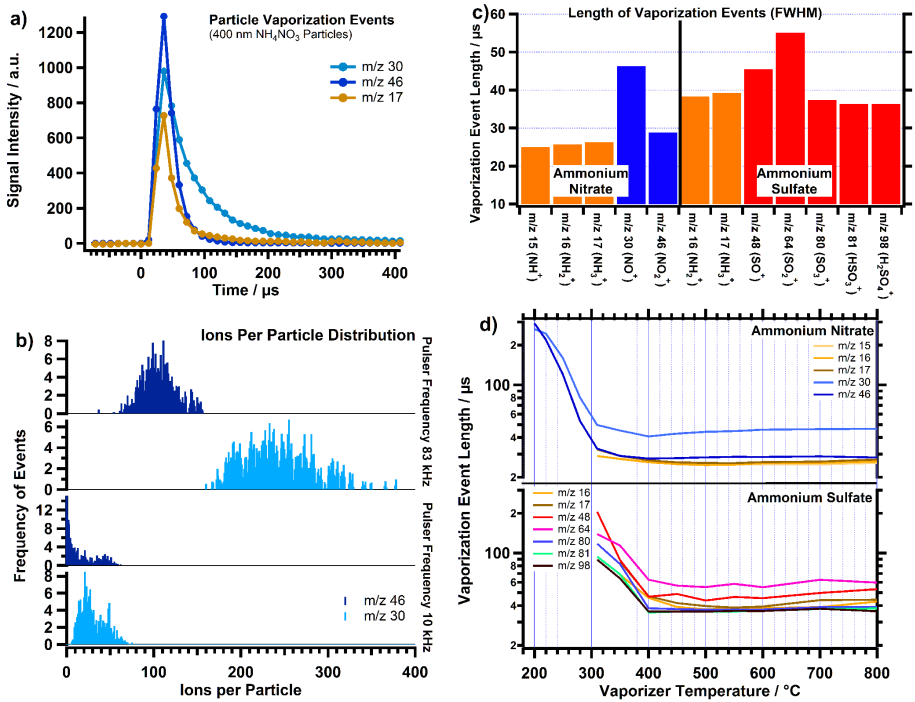

Figure 2. Single particle vaporization event measurements. **(a)** Average single particle vaporization events as measured for various ions from NH_4NO_3 (approx. 100 events averaged). **(b)** Ions per particle distribution for m/z 30 and 46 measured for 400 nm NH_4NO_3 particles with two different ToF-MS pulser frequencies (83 and 10 kHz, respectively). **(c)** Vaporization event lengths (FWHM) for ions from NH_4NO_3 and $(NH_4)_2SO_4$. **(d)** Vaporization event lengths for ions from NH_4NO_3 and $(NH_4)_2SO_4$ as a function of vaporizer temperature. The uncertainty of event lengths is ~ 10 %.

AMTD
8, 3525–3570, 2015

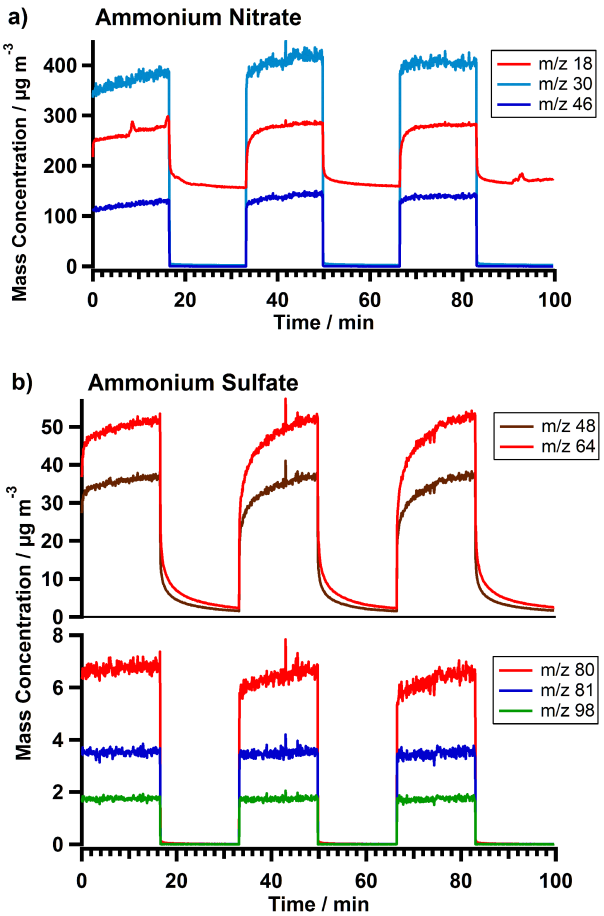

Figure 3. Time-resolved concentrations of ions from measurements of NH_4NO_3 **(a)** and $(NH_4)_2SO_4$ **(b)** for extended aerosol beam (*beam open*) and instrument background (*beam closed*) measurements. Precision of the measurements is < 10 %.

AMTD
8, 3525–3570, 2015

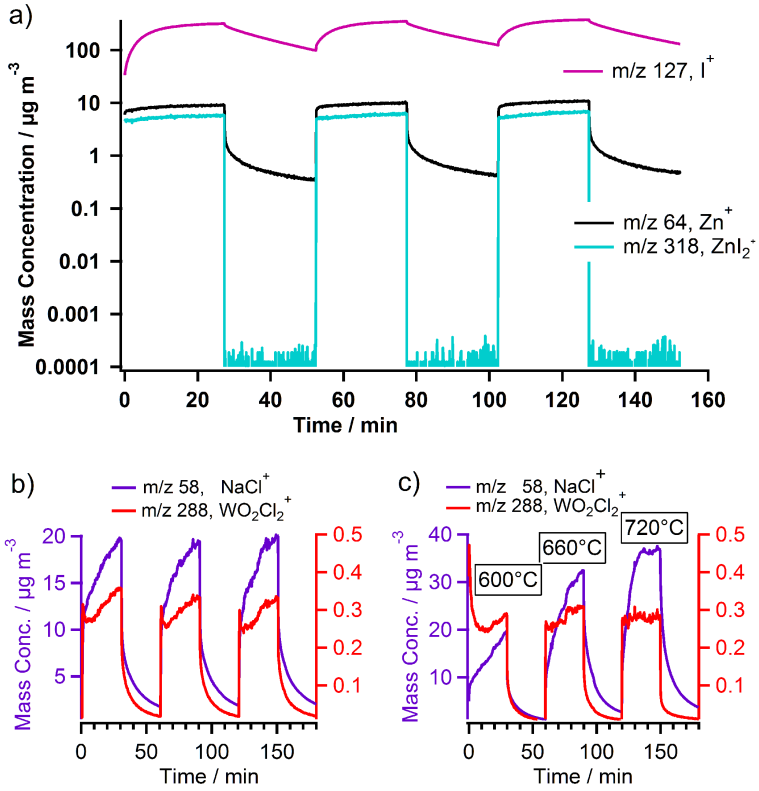

Figure 4. Time-resolved signal intensities for ions from measurements of ZnI_2 **(a)** and NaCl **(b, c)**. In **(b, c)** the left axis is for $NaCl^+$, the right axis is for $WO_2Cl_2^+$. The measurements in **(a)** and **(b)** were performed at constant vaporizer temperature of 600 °C, the measurements in **(c)** were performed at vaporizer temperatures of 600, 660, and 720 °C. Precision of the measurements is < 10 %.

AMTD
8, 3525–3570, 2015

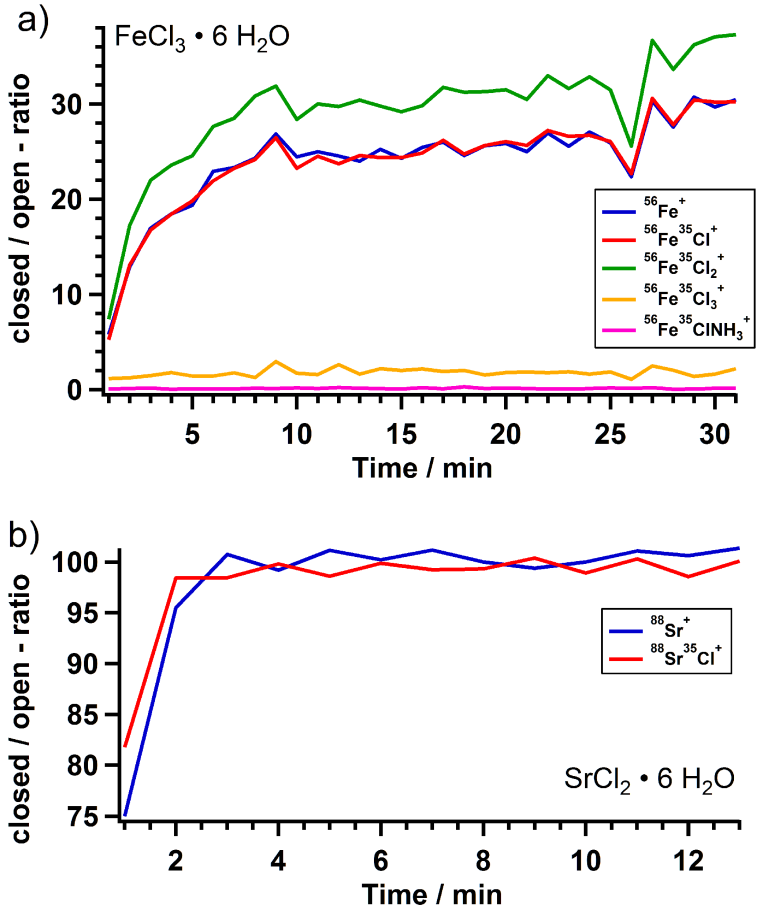

Figure 5. Ratio of instrument background/aerosol beam measurement intensity (c/o ratio, in percent) for ions from $FeCl_3 \cdot 6H_2O$ and from $SrCl_2 \cdot 6H_2O$ for the first minutes of aerosol measurement. Precision of the measurements is < 15 %.

AMTD
8, 3525–3570, 2015

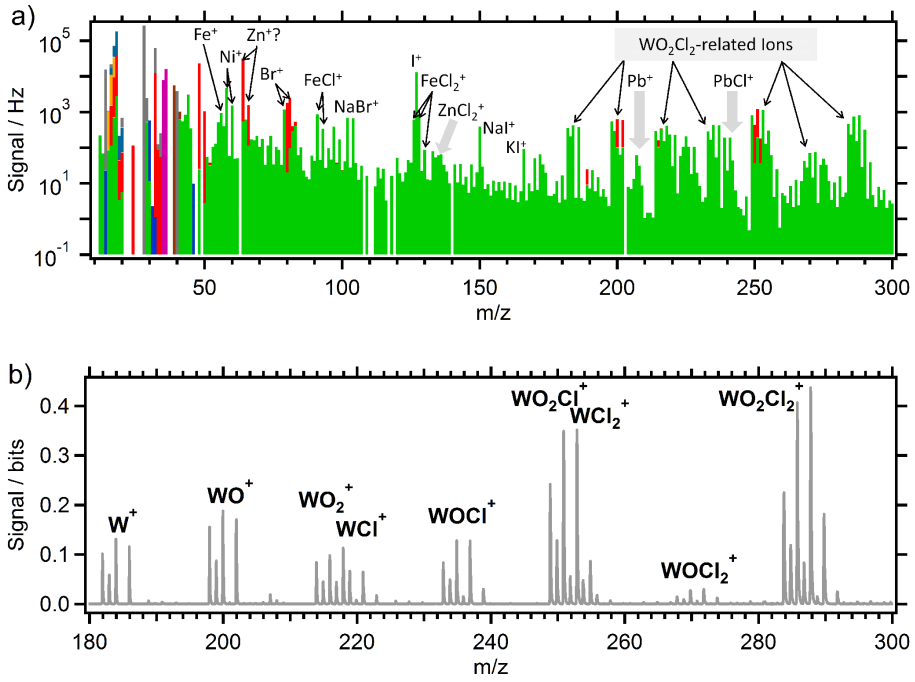

Figure 6. (a) One-minute average unit-mass resolution mass spectrum from a measurement of the exhaust aerosol of a municipal waste incinerator (ammonium: orange, nitrate: blue, sulfate: red, chloride: purple, organics: green; association of ion signals from the standard frag table). **(b)** Cutout of the high-resolution mass spectrum of **(a)** showing the WO_2Cl_2-related ion signals.

AMTD
8, 3525–3570, 2015

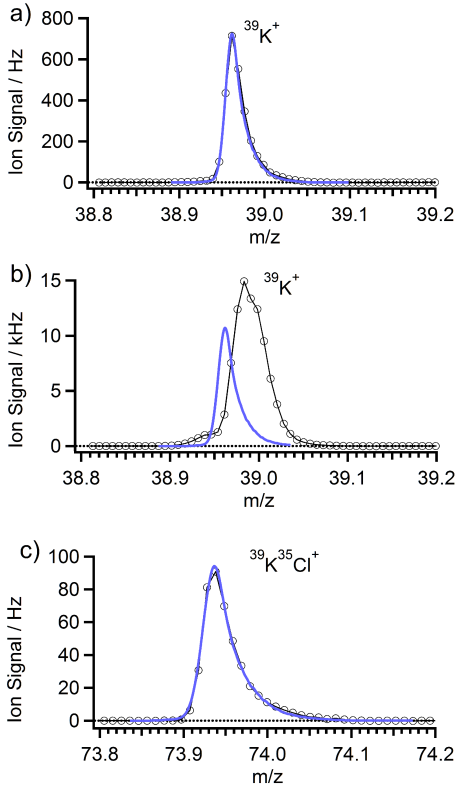

Figure 7. High-resolution mass spectra from the measurement of KCl. Measured data are shown as black markers and traces; blue traces are fits to the data with pre-defined peak positions, shapes and widths according to the expected ion signal. **(a)** The m/z 39 ($^{39}K^+$) ion peak at the beginning of the measurement day. **(b)** The m/z 39 ($^{39}K^+$) ion peak at the end of the measurement day. **(c)** The m/z 74 ($^{39}K^{35}Cl^+$) ion peak at the end of the measurement day.

AMTD
8, 3525–3570, 2015